

Accepted Manuscript

Paleomagnetic data from the New England Orogen (eastern Australia) and implications for oroclinal bending

Uri Shaanan, Gideon Rosenbaum, Sergei Pisarevsky, Fabio Speranza

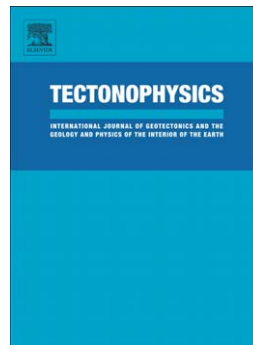
PII: S0040-1951(15)00519-3
DOI: doi: [10.1016/j.tecto.2015.09.018](https://doi.org/10.1016/j.tecto.2015.09.018)
Reference: TECTO 126785

To appear in: *Tectonophysics*

Received date: 3 July 2015
Revised date: 12 September 2015
Accepted date: 15 September 2015

Please cite this article as: Shaanan, Uri, Rosenbaum, Gideon, Pisarevsky, Sergei, Speranza, Fabio, Paleomagnetic data from the New England Orogen (eastern Australia) and implications for oroclinal bending, *Tectonophysics* (2015), doi: [10.1016/j.tecto.2015.09.018](https://doi.org/10.1016/j.tecto.2015.09.018)

This is a PDF file of an unedited manuscript that has been accepted for publication. As a service to our customers we are providing this early version of the manuscript. The manuscript will undergo copyediting, typesetting, and review of the resulting proof before it is published in its final form. Please note that during the production process errors may be discovered which could affect the content, and all legal disclaimers that apply to the journal pertain.



**Paleomagnetic data from the New England Orogen (eastern Australia)
and implications for oroclinal bending**

Uri Shaanan¹, Gideon Rosenbaum¹, Sergei Pisarevsky^{2,3} and Fabio Speranza⁴

¹ School of Earth Sciences, The University of Queensland, Brisbane, Queensland,
Australia

² School of Earth and Environment, University of Western Australia, Crawley, Western
Australia, Australia

³ The Institute for Geoscience Research (TIGeR), Department of Applied Geology,
Curtin University of Technology, Perth, Western Australia, Australia

⁴ Istituto Nazionale di Geofisica e Vulcanologia, Rome, Italy

Corresponding author (Uri Shaanan) email: u.shaanan@uq.edu.au

ABSTRACT

Orogenic curvatures (oroclines) are common in modern and ancient orogens, but the geodynamic driving forces of many oroclines remain controversial. Here we focus on the New England oroclines of eastern Australia, the formation of which had been previously broadly constrained to the Early-Middle Permian. This time interval encompasses periods of both back-arc extension (at ~300-280 Ma) and subsequent contractional deformation (Hunter-Bowen Orogeny) that commenced at ~270 Ma along the paleo-Pacific and Gondwanan subduction plate boundary. We present new paleomagnetic data from volcanic rocks that were extruded during the transition from extension to contraction (at ~272 Ma), and we show that the oroclinal structure must have formed prior to the emplacement of the volcanic rocks. Our results thus indicate that oroclinal bending in the southernmost New England Orogen has been completed prior to the onset of Middle Permian contractional deformation. It is therefore concluded that the oroclines have likely formed during back-arc extension, and that a major contribution to the orogenic curvature was driven by trench retreat.

Keywords: Oroclinal bending, Subduction rollback, Back-arc extension, New England Orogen, Paleomagnetism.

1. INTRODUCTION

Two competing hypotheses are commonly invoked to explain the origin of oroclinal bending. Some researchers link the formation of thick-skinned oroclinal bending to orogen-parallel compression (Fig. 1a) and buckling of the whole lithosphere (e.g., Gutiérrez-Alonso et al., 2004; Johnston et al., 2013; Weil et al., 2013). Other models assume that oroclinal bending is primarily controlled by orogen-perpendicular forces (Fig. 1b) imposed by processes such as indentation and subduction rollback (e.g., Moresi et al., 2014; Rosenbaum, 2014). In many of the latter models, oroclinal bending has occurred contemporaneously with back-arc extension in response to trench retreat (e.g., Royden, 1993; Lonergan and White, 1997; Maffione et al., 2013). In these types of oroclinal bending, which are common, for example, in the Mediterranean region (Rosenbaum, 2014), oroclinal bending does not seem to be associated with orogen-parallel buckling. However, in many other orogenic systems, temporal relationships between intermitted periods of extension, contraction, block translation, and oroclinal bending are not well constrained. In this paper, we establish these relationships for a set of late Paleozoic oroclinal bending in the southern New England Orogen, eastern Australia (Fig. 2), and use our findings to demonstrate intimate links between oroclinal bending and back-arc extension.

Constraints on the timing of oroclinal bending in the New England Orogen indicate that the oroclinal bending formed during the Early to Middle Permian (~300-260 Ma, e.g., Rosenbaum et al., 2012). This time interval overlaps with both a major phase of extensional tectonism that occurred in eastern Australia at ~300-280 Ma (Fig. 3; Korsch et al., 2009a), as well as with the initiation of subsequent contractional deformation

that affected the region between ~270 to 230 Ma (Hunter-Bowen Orogeny, Fig. 3; Collins, 1991; Holcombe et al., 1997). Previous constraints on the timing of oroclinal bending were therefore insufficient for determining whether the New England oroclines formed during the early phase of extension or in the course of the subsequent phase of contraction, thus impeding our ability to understand the dynamics of oroclinal bending. To resolve this problem, we conducted a paleomagnetic study on volcanic rocks (Alum Mountain Volcanics, Fig. 4) that were emplaced at ~272 Ma (Roberts et al., 1996; Li et al., 2014), i.e., at the transitional period between extension to contraction. A comparison of our results with contemporary paleomagnetic data from Gondwana provides a robust constraint on the timing of oroclinal bending and an insight into the geodynamics of orocline formation in eastern Australia.

2. GEOLOGICAL SETTING

The New England Orogen is the youngest and easternmost orogen in Australia (Fig. 2a, Glen, 2005). It is mainly composed of Devonian-Carboniferous supra-subduction rocks associated with a west-dipping (present day orientation) subduction zone (Leitch, 1974), which were intruded by Permian-Triassic magmatic rocks (Shaw and Flood, 1981). In the southern New England Orogen, the Devonian-Carboniferous rocks are predominantly associated with a fore-arc region, and include fore-arc basin strata (Tamworth Belt and correlative blocks) and accretionary complex units (Fig. 2b, Leitch, 1974). The Early Permian rocks in the southern New England Orogen are dominated by

S-type granitoids and clastic sedimentary successions, which were likely deposited in a back-arc extensional setting (Holcombe et al., 1997; Korsch et al., 2009a; Shaanan et al., 2015). Collectively, a number of geological observations suggest that from ~300 Ma to ~280 Ma, the New England Orogen was positioned in an extensional back-arc setting (Fig. 3a, c, and corresponding references). Firstly, during this period widespread sedimentary basins were developed, most notably in the Sydney, Gunnedah and Bowen basins (Fig. 2), with evidence that basin formation was accompanied by extensional faulting (Korsch et al., 2009a). Basin formation involved bimodal volcanism, including the possible emplacement of a 4.5–9 km succession of mafic rift-related volcanic rocks (Meandarra Gravity Ridge, Fig. 3a) beneath the Permian strata (Krassay et al., 2009). Secondly, evidence for crustal melting and the emplacement of 298–288 Ma S-type granitoids (Jeon et al., 2012; Rosenbaum et al., 2012), as well as coeval local high-temperature metamorphism (Craven et al., 2012), indicates that the heat flow during this period was relatively high. This is a characteristic feature of back-arc regions (Currie and Hyndman, 2006). The transition from a fore-arc region during the Carboniferous to a back-arc environment in the Early Permian was attributed to the onset of eastward trench retreat (Jenkins et al., 2002; Shaanan et al., 2015).

The initiation of the Hunter-Bowen Orogeny, at ~270 or ~265 Ma (Fig. 3; Collins, 1991; Holcombe et al., 1997) marked an abrupt change in the style of tectonism throughout the New England Orogen. Contractual deformation produced folds and thrusts (Fig. 3b, c, and corresponding references), and affected Lower Permian rocks of the Sydney, Gunnedah and Bowen basins, which evolved into a foreland system (Fergusson, 1991; Fielding et al., 1997; Korsch and Totterdell, 2009; Korsch et al., 2009a; Korsch et al.,

2009b). The shift from regional extension and high heat flow to a contractional fold-and-thrust belt coincides with a general quiescence in the regional magmatism, from ~280 to ~260 Ma, with the exception of ~271-266 Ma volcanism in the southernmost New England Orogen, which includes the Alum Mountain Volcanics. The REE pattern of the Alum Mountain Volcanics suggests that it was derived primarily from a depleted upper asthenosphere, and accordingly, the origin of these volcanic rocks has been hypothesized to indicate an episode of slab break-off (Caprarelli and Leitch, 2001; Li et al., 2014).

Widespread magmatism throughout the southern New England Orogen recommenced at ~260 Ma and continued until ~220 Ma (Fig. 3c). Unlike the earlier phase of mostly S-type granitoids, the Late Permian to Triassic phase of magmatic activity predominantly involved the emplacement of I-type granitoids and calc-alkaline volcanism (Fig. 3c; Shaw and Flood, 1981; Bryant et al., 1997).

The most prominent deformational feature within the southern New England Orogen is a set of tight oroclines that include the Z-shaped Texas and Coffs-Harbour oroclines in the north and the S-shaped Manning and Nambucca oroclines in the south (Fig. 2b). Evidence for the existence of these oroclines includes (1) a curved belt of early Paleozoic serpentinites (Korsch and Harrington, 1987), (2) curved structural and magnetic fabrics within the Devonian-Carboniferous subduction complex (Korsch and Harrington, 1987; Aubourg et al., 2004; Li et al., 2012; Li and Rosenbaum, 2014; Mochales et al., 2014), (3) the spatial distribution of the segmented Devonian-Carboniferous fore-arc basin blocks (Korsch and Harrington, 1987; Glen and Roberts, 2012; Rosenbaum, 2012; Hoy et al., 2014) and (4) a curved belt of deformed S-type

Early Permian granitoids (Fig. 2b; Rosenbaum et al., 2012). The age of the Early Permian granitoids (298-288 Ma) provides a maximum constraint for the timing of oroclinal bending, whereas a minimum age constraint is provided by the occurrence of the Late Permian to Triassic (260-220 Ma) I-type magmatic rocks that crosscut the oroclinal structure (Cawood et al., 2011b; Rosenbaum et al., 2012).

Paleomagnetic data from Lower Carboniferous fore-arc basin strata (Rouchel, Gresford and Myall blocks; Fig. 2b) were interpreted as an indication for counterclockwise rotations of 80° for the Rouchel and Gresford blocks and 120° for the Myall Block, around vertical axes located within these blocks (Geeve et al., 2002), or for more modest rotations around distal vertical axes (Cawood et al., 2011b). Within the Myall Block, Permian strata are exposed in the cores of two north-south trending, doubly-plunging synclines (Gloucester and Myall; Figs. 2b, 4). These folds are thought to have formed in response to ~E-W Hunter-Bowen contractional deformation, and a subsequent phase of contraction that produced a Type-1 fold interference pattern (Korsch and Harrington, 1981; Collins, 1991). The folded succession includes Permian clastic sedimentary rocks underlain by a volcanic horizon (the Alum Mountain Volcanics), which unconformably overlies the Carboniferous fore-arc basin rocks (Fig. 4c, d).

Exposures of the Alum Mountain Volcanics form an oval ridge that highlights the structure of the Gloucester syncline (Fig. 4). Both the thickness and composition of the Alum Mountain Volcanics are variable. The maximum thickness is 1800 meters and the lithology includes basalt, andesite, dacite, rhyolite flows, breccias, welded-ash flows and ash-fall tuffs (Carey and Browne, 1938; Roberts et al., 1991; Caprarelli and Leitch,

2001). The age of the Alum Mountain Volcanics has been dated at 271.8 ± 1.8 Ma using $^{40}\text{Ar}/^{39}\text{Ar}$ geochronology (Li et al., 2014), and 274.1 ± 3.4 Ma using U–Pb SHRIMP zircon geochronology (Roberts et al., 1996).

3. METHODS

We conducted petrographic, structural, and paleomagnetic investigation of the Alum Mountain Volcanics. Oriented samples from 25 localities in the Myall Block (Fig. 4a) were drilled using a hand held Pomeroy EZ Core Drill model D261-C. Cores were oriented, using Pomeroy orienting fixture, with a magnetic compass, and when possible a sun compass. The top and bottoms of the sampled cores were trimmed in the laboratory, and 22 mm long cylindrical specimens were separated for measurements. Tilt correction for paleomagnetic sampling sites were based on structural constraints from proximal overlying sedimentary strata (Fig. 4a). Magnetic measurements were carried out in a magnetically shielded room with a DC-SQUID cryogenic magnetometer at the Istituto Nazionale di Geofisica e Vulcanologia (INGV, Rome, Italy). Samples were stepwise demagnetized using thermal up to 680°C and alternating field (AF) up to 130 mT techniques. Data analyses were conducted using Remasoft 3.0 (Chadima and Hrouda, 2006) and IAPD (Torsvik, 1986) software.

4. RESULTS

4.1. Petrography and structural data

The composition and degrees of alteration of the Alum Mountain Volcanics were found to be extremely variable even within outcrops. Samples consisted of basalt, trachyte, quartz rhyolite and ignimbrite (Fig. 5). The more mafic lithologies include amygdaloids and fractures filled by pumpellyite (Fig 5a), indicating a low prehnite-pumpellyite metamorphic facies (temperatures of ~100-300°C). The absence of actinolite and epidote and the presence of chlorite, quartz and calcite, are consistent with the suggestion that metamorphic conditions were lower than greenschist facies.

Analyses of structural data were restricted to strata from above the Permian-Carboniferous unconformity. Projection of 165 poles to bedding from across the Gloucester syncline shows a scatter attributed to non-cylindrical folding (Fig. 4b). These data can be subdivided into northern, central and southern domains. The structure of the northern domain is characterized by an upright rounded fold with a shallow south plunging hinge ($\beta_n = 04/190$; Fig. 4b, d), whereas the fold in the southern domain is angular and plunges moderately to the north ($\beta_s = 18/359$; Fig. 4b, c). This double-plunging fold geometry was used for calculating the paleomagnetic tilt-correction.

4.2. Paleomagnetism

The Natural Remanent Magnetization (NRM) of the Alum Mountain Volcanics varies strongly from 0.9 mA/m to 2.5 A/m. Both AF and thermal stepwise demagnetizations have been applied (Fig. 6a, b). In some cases, where full

demagnetization was not achieved by 100-130 mT alternating field, samples were thermally demagnetized at 400-680°C (e.g., Fig. 6c). Samples from eight sites either do not carry a stable remanence magnetization, or have highly scattered ($\alpha_{95} > 16^\circ$) and/or inconsistent (within site) characteristic remanence directions (Fig. 4a). These sites include the most altered lithologies mentioned above and were excluded from further analysis.

Most other samples carry a stable steep downward (after tilt correction) unipolar characteristic remanent magnetization, which is likely carried by magnetite and/or hematite (Figs. 6 and 7b; Table 1). Few samples have an additional low-stability, randomly-oriented remanence component, which was removed after the first few steps of demagnetization. The characteristic remanence directions from the 18 prospective sites are scattered in geographic coordinates, but the scatter decreases significantly when a tilt correction is applied (Fig. 7a, b). The fold test of McFadden (1990) is positive at the 99% confidence level; fold test SCOS values are 9.447 in situ and 1.517 after tilt correction with critical value of 6.919. The in situ Fisher's precision parameter is 1.5 and after tilt correction is 10.7 (Fig. 7). We therefore conclude that the measured remanent magnetization is pre-folding. The overall tilt-corrected remanence direction is $D=27.5^\circ$, $I=88.2^\circ$ ($N=18$, $k=10.7$, $\alpha_{95}=11.1^\circ$) and the corresponding paleomagnetic pole is at 30.0°S , 153.2°E ($A_{95} = 19.5^\circ$).

5. DISCUSSION

5.1. Data interpretation

The positive paleomagnetic fold test (Fig. 7) indicates that the analyzed characteristic magnetization component of the Alum Mountain Volcanics predates folding in the Gloucester and Myall synclines. The low temperatures of the sub-greenschist metamorphic conditions ($<300^{\circ}\text{C}$) makes the possibility of re-magnetization less likely, and in conjunction with the positive fold test, suggests that the measured characteristic magnetization is primary.

Previously published paleomagnetic data from the New England Orogen were compiled by Cawood et al. (2011b), who proposed a model that involved buckling and significant northward translations, possibly assisted by sinistral strike-slip faulting. However, the timing and mechanism of oroclinal bending have remained poorly constrained, particularly because paleomagnetic data from the southern New England Orogen were limited to older rocks (Devonian and Carboniferous) in comparison to the Permian rocks sampled by us. Therefore, the timing of the final stage of oroclinal bending has remained unconstrained. A comparison of our calculated ~ 272 Ma paleopole of the Myall Block (30.0°S , 153.2°E , $\alpha_{95}=19.5^{\circ}$) with the mean 275-270 Ma Gondwanan pole (recalculated from McElhinny et al., 2003 and Cawood et al., 2011b) and with the mean pole for the northern Tamworth Belt (Schmidt, 1988; Lackie and Schmidt, 1993; Opdyke et al., 2000; Klootwijk, 2002, 2003; summarized by Cawood et al., 2011b) shows overlapping confidence circles. This indicates that at ~ 272 Ma the Myall Block was located close to its present position with respect to cratonic Australia (Fig. 8a).

The proximity and overlap in confidence circles of the paleopoles suggests that by ~272 Ma, the blocks of the New England Orogen were close to their present-day position with respect to cratonic Australia (Gondwana), hence that the oroclinal structure was predominantly complete. When plotting the blocks in their exact current arrangement with respect to Australia, the confidence circles of the Gondwanan and Tamworth Belt poles are close but do not overlap (Fig. 8b), indicating that a minor component of relative translation postdated the Early Permian. As indicated by our positive fold test, the formation of Gloucester and Myall synclines is an example for deformation that occurred after ~272 Ma. These folds and inferred translations are likely related to contractional deformation during the Hunter-Bowen Orogeny (Fig. 3) and though it may have affected the overall oroclinal structure, our data indicate that oroclinal bending in the southernmost New England Orogen (Manning Orocline) was essentially completed prior to the initiation of the Hunter-Bowen Orogeny.

5.2. Timing and tectonic setting of oroclinal bending in the New England Orogen

Previous suggestions for the timing of oroclinal bending, based on hitherto available constraints, broadly ranged from (a) Middle to Late Carboniferous (Murray et al., 1987; Geeve et al., 2002), and (b) latest Carboniferous (or earliest Permian) to Middle Permian (~305-260 Ma; Cawood et al., 2011b; Glen and Roberts, 2012; Rosenbaum et al., 2012), and (c) Late Permian (Collins et al., 1993). Whether the northern oroclinal (Texas and Coffs Harbour oroclinal) developed simultaneously with the southern oroclinal (Manning and Nambucca oroclinal) is unknown. However, both sets of structures show evidence for a curved belt of Early Permian granitoids (298-288 Ma), which mimics the geometry of the oroclinal, thus indicating that both the northern

and southern oroclinal bends formed during or after the emplacement of these granitoids (Rosenbaum et al., 2012). Our new paleomagnetic results further constrain the timing of oroclinal bending, indicating that the southern part of the New England oroclinal bend (i.e., Manning Orocline) must have developed prior to the emplacement of the Alum Mountain Volcanics at ~272 Ma. Therefore, the Manning Orocline must have formed in the Early Permian after ~298 Ma and before ~272 Ma. Importantly, this time span predated the initiation of contractional deformation associated with the Hunter-Bowen Orogeny (Fig. 3).

The collective geological evidence for Early Permian contemporaneous emplacement of S-type granitoids, high-temperature metamorphism, and extensional faulting (Fig. 3, and corresponding references), indicate that during this period, the New England Orogen was positioned in a hot back-arc extensional setting (Jenkins et al., 2002; Korsch et al., 2009a; Shaanan et al., 2015). Furthermore, age spectra of detrital zircons from the Early Permian Nambucca Block (Fig. 2b), include a major component of pre-Devonian ages, implying that detritus was derived from cratonic Australia (Gondwana), as expected for a sedimentary basin that was positioned in a back-arc setting (Shaanan et al., 2015). The new time constraint for the formation of the Manning Orocline, therefore, indicates that oroclinal bending took place when the whole area was situated in an extensional back-arc setting.

5.3. Implications for the geodynamics of oroclinal bending

The constraints on the timing of oroclinal bending in the southernmost New England Orogen, in conjunction with evidence for contemporaneous back-arc extension, raise

the possibility that trench retreat played an important role in the formation of the New England oroclinal. Trench retreat is controlled by the negative buoyancy of subducting slabs relative to surrounding asthenosphere, and by the flux of mantle return flow that volumetrically compensates the retrograde slab motion (Elsasser, 1971; Garfunkel et al., 1986). Lateral variations in the rate of trench retreat are common (Jarrard, 1986; Schellart et al., 2007), and are responsible for the formation of arcuate segments and cusps in the geometry of plate boundaries (Schellart and Lister, 2004; Morra et al., 2006; Schellart et al., 2007). In particular, higher retreat rates and tighter curvatures have been shown to occur in the proximity of the slab edges and in response to subduction of narrow slab segments (Stegman et al., 2006; Schellart et al., 2007). As demonstrated in numerous examples in modern tectonics, such a progressive formation of plate boundary curvatures is intimately linked to the development of back-arc extensional basins and block rotations in the overriding plate (Lonergan and White, 1997; Rosenbaum and Lister, 2004; Faccenna et al., 2014; Rosenbaum, 2014). Accordingly, rotation and translation of blocks and tectonic nappes in the overriding plate, in response to the development of plate boundary curvatures, can result in the formation of oroclinal.

The suggestion that oroclinal form in response to plate boundary migration (e.g., trench retreat or indentation) is fundamentally different from the type of processes proposed, for example, for the origin of the (Paleozoic) Cantabrian Orocline (Weil et al., 2013) or Kazakhstan Orocline (Xiao et al., 2010). Most models for the formation of these oroclinal assume that bending occurred through buckling of the whole lithosphere in response to orogen-parallel contraction (Fig. 1a), but whether this

process is geodynamically plausible is yet to be demonstrated. Moreover, modern oroclinal bends, for example, in the Mediterranean region (Rosenbaum, 2014), eastern Indonesia (Hall, 2012) and southwest Pacific (Schellart et al., 2006), do not show evidence for lithospheric buckling, and appear to be primarily controlled by a combination of continental indentation and trench retreat (Fig. 1b). It is therefore possible that the role of buckling has been overestimated in reconstructions of ancient oroclinal bends.

Results of this study suggest that similarly to some modern examples, oroclinal bending in the southernmost New England Orogen was driven by trench retreat. The evidence for extensional tectonism during the Early Permian, together with the indication that oroclinal bending was mostly concluded prior to the commencement of the Hunter-Bowen Orogeny, are consistent with the suggestion that trench retreat accompanied by back-arc extension, rather than orogen-parallel contraction, was the primary mechanism that controlled oroclinal bending in the New England Orogen.

6. CONCLUSIONS

New paleomagnetic data indicate that the southern part of the New England oroclinal bends predominantly formed in the Early Permian, before ~272 Ma. During this period, the former (Devonian-Carboniferous) fore-arc units of the New England Orogen were positioned in an extensional back-arc setting, indicating that a substantial migration of the subduction boundary must have occurred. The established spatial and temporal link between the formation of the Manning Orocline with back-arc extension and the migration of the subduction boundary, suggest that similarly to modern examples such

as the Mediterranean region, the formation of the New England oroclinal was primarily controlled by trench retreat.

7. ACKNOWLEDGMENTS

This work was funded by the Australian Research Council (grant DP130100130). We thank Llyam White for field assistance, Derek Hoy for fruitful discussions and Tania Mochales López for technical assistance. TIGeR publication #637.

8. REFERENCES CITED

- Allen, C.M., 2000. Evolution of a post-batholith dike swarm in central coastal Queensland, Australia: arc-front to backarc? *Lithos* 51, 331-349.
- Allen, C.M., Williams, I.S., Stephens, C.J., Fielding, C.R., 1998. Granite genesis and basin formation in an extensional setting: The magmatic history of the northernmost New England Orogen. *Australian Journal of Earth Sciences* 45, 875-888.
- Aubourg, C., Klootwijk, C., Korsch, R.J., 2004. Magnetic fabric constraints on oroclinal bending of the Texas and Coffs Harbour blocks: New England Orogen, eastern Australia, in: Martín-Hernández, F., Lüneburg, C.M., Aubourg, C., Jackson, M. (Eds.), *Magnetic Fabric: Methods and Applications*. Geological Society, London, Special Publications, pp. 421-445.
- Brooke-Barnett, S., Rosenbaum, G., 2015. Structure of the Texas Orocline beneath the sedimentary cover (southeast Queensland, Australia). *Australian Journal of Earth Sciences* 62, 425-445.

- Bryant, C.J., Arculus, R.J., Chappell, B.W., 1997. Clarence River supersuite: 250 Ma cordilleran tonalitic I-type intrusions in eastern Australia. *Journal of Petrology* 38, 975-1001.
- Caprarelli, G., Leitch, E.C., 1998. Magmatic changes during the stabilisation of a cordilleran fold belt: the Late Carboniferous–Triassic igneous history of eastern New South Wales, Australia. *Lithos* 45, 413-430.
- Caprarelli, G., Leitch, E.C., 2001. Geochemical evidence from Lower Permian volcanic rocks of northeast New South Wales for asthenospheric upwelling following slab breakoff. *Australian Journal of Earth Sciences* 48, 151-166.
- Carey, S.W., Browne, W.R., 1938. Review of the Carboniferous stratigraphy, tectonics and palaeogeography of New South Wales and Queensland. *Journal and Proceedings of the Royal Society of New South Wales* 71, 591-614.
- Cawood, P.A., 2005. Terra Australis Orogen: Rodinia breakup and development of the Pacific and Iapetus margins of Gondwana during the Neoproterozoic and Paleozoic. *Earth-Science Reviews* 69, 249-279.
- Cawood, P.A., Leitch, E.C., Merle, R.E., Nemchin, A.A., 2011a. Orogenesis without collision: Stabilizing the Terra Australis accretionary orogen, eastern Australia. *Geological Society of America Bulletin* 123, 2240-2255.
- Cawood, P.A., Pisarevsky, S.A., Leitch, E.C., 2011b. Unraveling the New England orocline, east Gondwana accretionary margin. *Tectonics* 30, TC5002.
- Chadima, M., Hroudá, F., 2006. Remasoft 3.0 paleomagnetic data browser and analyzer. Agico, Inc., Czech Republic.

- Collins, W.J., 1991. A reassessment of the 'Hunter-Bowen Orogeny': Tectonic implications for the southern New England fold belt. *Australian Journal of Earth Sciences* 38, 409-423.
- Collins, W.J., Offler, R., Farrell, T.R., Landenberger, B., 1993. A revised Late Palaeozoic-Early Mesozoic tectonic history for the southern New England Fold Belt, in *New England Orogen, eastern Australia*. Department of Geology and Geophysics, University of New England, Armidale.
- Craven, S.J., Daczko, N.R., Halpin, J.A., 2012. Thermal gradient and timing of high-T–low-P metamorphism in the Wongwibinda Metamorphic Complex, southern New England Orogen, Australia. *Journal of Metamorphic Geology* 30, 3-20.
- Currie, C.A., Hyndman, R.D., 2006. The thermal structure of subduction zone back arcs. *Journal of Geophysical Research* 111, B08404.
- Elsasser, W.M., 1971. Sea-floor spreading as thermal convection. *Journal of Geophysical Research* 76, 1101-1112.
- Faccenna, C., Becker, T.W., Auer, L., Billi, A., Boschi, L., Brun, J.P., Capitanio, F.A., Funicello, F., Horvath, F., Jolivet, L., Piromallo, C., Royden, L., Rossetti, F., Serpelloni, E., 2014. Mantle dynamics in the Mediterranean. *Reviews of Geophysics* 52, 2013RG000444.
- Fergusson, C.L., 1991. Thin-skinned thrusting in the northern New England Orogen, central Queensland, Australia. *Tectonics* 10, 797-806.
- Fergusson, C.L., Henderson, R.A., Leitch, E.C., 1990. Structural history and tectonics of the Palaeozoic Shoalwater and Wandilla terranes, northern New England Orogen, Queensland. *Australian Journal of Earth Sciences* 37, 387-400.

- Fergusson, C.L., Henderson, R.A., Leitch, E.C., Ishiga, H., 1993. Lithology and structure of the Wandilla terrane, Gladstone-Yeppoon district, central Queensland, and an overview of the Palaeozoic subduction complex of the New England Fold Belt. *Australian Journal of Earth Sciences* 40, 403-414.
- Fielding, C.R., Stephens, C.J., Holcombe, R.J., 1997. Submarine mass-wasting deposits as an indicator of the onset of foreland thrust loading—Late Permian Bowen Basin, Queensland, Australia. *Terra Nova* 9, 14-18.
- Flood, R.H., Shaw, S.E., 1977. Two "S-type" granite suites with low initial $^{87}\text{Sr}/^{86}\text{Sr}$ ratios from the New England Batholith, Australia. *Contributions to Mineralogy and Petrology* 61, 163-173.
- Garfunkel, Z., Anderson, C.A., Schubert, G., 1986. Mantle circulation and the lateral migration of subducted slabs. *Journal of Geophysical Research* 91, 7205-7223.
- Geeve, R.J., Schmidt, P.W., Roberts, J., 2002. Paleomagnetic results indicate pre-Permian counter-clockwise rotation of the southern Tamworth Belt, southern New England Orogen, Australia. *Journal of Geophysical Research* 107.
- Glen, R.A., 2005. The Tasmanides of eastern Australia, in: Vaughan, A.P.M., Leat, P.Y., Pankhurst, R.J. (Eds.), *Terrane Processes at the Margins of Gondwana*. Geological Society of London Special Publication, pp. 23-96.
- Glen, R.A., Roberts, J., 2012. Formation of oroclinal in the New England Orogen, eastern Australia. *Journal of the Virtual Explorer* 43, 1-38.
- Gutiérrez-Alonso, G., Fernández-Suárez, J., Weil, A.B., 2004. Orocline triggered lithospheric delamination. *Geological Society of America Special Papers* 383, 121-130.

- Hall, R., 2012. Late Jurassic–Cenozoic reconstructions of the Indonesian region and the Indian Ocean. *Tectonophysics* 570–571, 1-41.
- Hammond, R., 1987. The Bowen Basin, Queensland, Australia: an upper crustal extension model for its early history. Bureau of Mineral Resources, Geology and Geophysics, Canberra, pp. 131-142.
- Holcombe, R.J., Little, T.A., 1994. Blueschists of the New England Orogen: Structural development of the Rocksberg Greenstone and associated units near Mt Mee, southeastern Queensland. *Australian Journal of Earth Sciences* 41, 115-130.
- Holcombe, R.J., Stephens, C.J., Fielding, C.R., Gust, D., Little, T.A., Sliwa, R., Kassan, J., McPhie, J., Ewart, A., 1997. Tectonic evolution of the northern New England Fold Belt: The Permian-Triassic Hunter-Bowen event, in: Ashley, P.M., Flood, P.G. (Eds.), *Geological Society of Australia Special Publication*. Geological Society, Australia, pp. 52-65.
- Hoy, D., Rosenbaum, G., Wormald, R., Shaanan, U., 2014. Geology and geochronology of the Emu Creek Block (northern New South Wales, Australia) and implications for oroclinal bending in the New England Orogen. *Australian Journal of Earth Sciences* 61, 1109-1124.
- Jarrard, R.D., 1986. Relations among subduction parameters. *Reviews of Geophysics* 24, 217-284.
- Jenkins, R.B., Landenberger, B., Collins, W.J., 2002. Late Palaeozoic retreating and advancing subduction boundary in the New England Fold Belt, New South Wales. *Australian Journal of Earth Sciences* 49, 467-489.

- Jeon, H., Williams, I.S., Chappell, B.W., 2012. Magma to mud to magma: Rapid crustal recycling by Permian granite magmatism near the eastern Gondwana margin. *Earth and Planetary Science Letters* 319-320, 104-117.
- Johnston, S.T., Weil, A.B., Gutierrez-Alonso, G., 2013. Oroclines: Thick and thin. *Geological Society of America Bulletin* 125, 643-663.
- Klootwijk, C., 2002. Carboniferous palaeomagnetism of the Rocky Creek Block, northern Tamworth Belt, and the New England pole path. *Australian Journal of Earth Sciences* 50, 129-135.
- Klootwijk, C.T., 2003. Carboniferous palaeomagnetism of the Werrie Block, northwestern Tamworth Belt, and the New England pole path. *Australian Journal of Earth Sciences* 50, 865-902.
- Korsch, R.J., Harrington, H.J., 1981. Stratigraphic and structural synthesis of the New England Orogen. *Journal of the Geological Society of Australia* 28, 205-226.
- Korsch, R.J., Harrington, H.J., 1987. Oroclinal bending, fragmentation and deformation of terranes in the New England Orogen, eastern Australia, in: Leitch, E.C., Scheibner, E. (Eds.), *Terrane accretion and orogenic belts*. American Geophysical Union, Washington, DC, pp. 129-139.
- Korsch, R.J., Totterdell, J.M., 2009. Subsidence history and basin phases of the Bowen, Gunnedah and Surat basins, eastern Australia. *Australian Journal of Earth Sciences* 56, 335-353.
- Korsch, R.J., Totterdell, J.M., Cathro, D.L., Nicoll, M.G., 2009a. Early Permian east Australian rift system. *Australian Journal of Earth Sciences* 56, 381-400.

- Korsch, R.J., Totterdell, J.M., Fomin, T., Nicoll, M.G., 2009b. Contractional structures and deformational events in the Bowen, Gunnedah and Surat basins, eastern Australia. *Australian Journal of Earth Sciences* 56, 477-499.
- Krassay, A.A., Korsch, R.J., Drummond, B.J., 2009. Meandarra Gravity Ridge: Symmetry elements of the gravity anomaly and its relationship to the Bowen–Gunnedah–Sydney Basin System. *Australian Journal of Earth Sciences* 56, 355-379.
- Lackie, M.A., Schmidt, P.W., 1993. Remagnetisation of strata during the Hunter-Bowen orogeny. *Exploration Geophysics* 24, 269-274.
- Landenberger, B., Farrell, T.R., Offler, R., Collins, W.J., Whitford, D.J., 1995. Tectonic implications of Rb-Sr biotite ages for the Hillgrove Plutonic Suite, New England Fold Belt, N.S.W., Australia. *Precambrian Research* 71, 251-263.
- Leitch, E.C., 1974. The geological development of the southern part of the New England Fold Belt. *Australian Journal of Earth Sciences* 21, 133-156.
- Li, P., Rosenbaum, G., 2014. Does the Manning Orocline exist? New structural evidence from the inner hinge of the Manning Orocline (eastern Australia). *Gondwana Research* 25, 1599-1613.
- Li, P., Rosenbaum, G., Donchak, P.J.T., 2012. Structural evolution of the Texas Orocline, eastern Australia. *Gondwana Research* 22, 279-289.
- Li, P., Rosenbaum, G., Vasconcelos, P., 2014. Chronological constraints on the Permian geodynamic evolution of eastern Australia. *Tectonophysics* 617, 20-30.
- Li, P., Rosenbaum, G., Yang, J.H., Hoy, D., 2015. Australian-derived detrital zircons in the Permian-Triassic Gympie terrane (eastern Australia): Evidence for an autochthonous origin. *Tectonics* 34, 858-874.

- Little, T.A., Holcombe, R.J., Gibson, G.M., Offler, R., Gans, P.B., McWilliams, M.O., 1992. Exhumation of late Paleozoic blueschists in Queensland, Australia, by extension faulting. *Geology* 20, 231-234.
- Little, T.A., McWilliams, M.O., Holcombe, R.J., 1995. $^{40}\text{Ar}/^{39}\text{Ar}$ thermochronology of epidote blueschists from the North D'Aguilar Block, Queensland, Australia: Timing and kinematics of subduction complex unroofing. *Geological Society of America Bulletin* 107, 520-535.
- Loneragan, L., White, N., 1997. Origin of the Betic-Rif mountain belt. *Tectonics* 16, 504-522.
- Maffione, M., Speranza, F., Cascella, A., Longhitano, S.G., Chiarella, D., 2013. A $\sim 125^\circ$ post-early Serravallian counterclockwise rotation of the Gorgoglione Formation (southern Apennines, Italy): New constraints for the formation of the Calabrian Arc. *Tectonophysics* 590, 24-37.
- McElhinny, M.W., Powell, C.M., Pisarevsky, S.A., 2003. Paleozoic terranes of eastern Australia and the drift history of Gondwana. *Tectonophysics* 362, 41-65.
- McFadden, P.L., 1990. A new fold test for palaeomagnetic studies. *Geophysical Journal International* 103, 163-169.
- Mochales, T., Rosenbaum, G., Speranza, F., Pisarevsky, S.A., 2014. Unraveling the geometry of the New England oroclines (eastern Australia): Constraints from magnetic fabrics. *Tectonics*, 2013TC003483.
- Moresi, L., Betts, P.G., Miller, M.S., Cayley, R.A., 2014. Dynamics of continental accretion. *Nature* 508, 245-248.
- Morra, G., Regenauer-Lieb, K., Giardini, D., 2006. Curvature of oceanic arcs. *Geology* 34, 877-880.

- Murray, C.G., Fergusson, C.L., Flood, P.G., Whitaker, W.G., Korsch, R.J., 1987. Plate tectonic model for the Carboniferous evolution of the New England Fold Belt. *Australian Journal of Earth Sciences* 34, 213-236.
- Offler, R., Foster, D.A., 2008. Timing and development of oroclinal bends in the southern New England Orogen, New South Wales. *Australian Journal of Earth Sciences* 55, 331-340.
- Opdyke, N.D., Roberts, J., Claoue-Long, J., Irving, E., Jones, P.J., 2000. Base of the Kiaman: Its definition and global stratigraphic significance. *Geological Society of America Bulletin* 112, 1315-1341.
- Powell, C.M., Li, Z.X., Thrupp, G.A., Schmidt, P.W., 1990. Australian Palaeozoic palaeomagnetism and tectonics—I. Tectonostratigraphic terrane constraints from the Tasman Fold Belt. *Journal of Structural Geology* 12, 553-565.
- Roberts, J., ClaoueLong, J.C., Foster, C.B., 1996. SHRIMP zircon dating of the Permian system of eastern Australia. *Australian Journal of Earth Sciences* 43, 401-421.
- Roberts, J., Engel, B., Chapman, J., 1991. Geology of the Camberwell, Dungog, and Bulahdelah 1:100 000 sheets 9133, 9233, 9333. Geological Survey of New South Wales, New South Wales.
- Rosenbaum, G., 2012. Oroclines of the southern New England Orogen, eastern Australia. *Episodes* 35, 187-194.
- Rosenbaum, G., 2014. Geodynamics of oroclinal bending: Insights from the Mediterranean. *Journal of Geodynamics* 82, 5-15.
- Rosenbaum, G., Li, P., Rubatto, D., 2012. The contorted New England Orogen (eastern Australia): New evidence from U-Pb geochronology of Early Permian granitoids. *Tectonics* 31, TC1006.

- Rosenbaum, G., Lister, G.S., 2004. Formation of arcuate orogenic belts in the western Mediterranean region, in: Sussman, A.J., Weil, A.B. (Eds.), *Orogenic curvature: Integrating paleomagnetic and structural analyses*. Geological Society of America Special Papers 383, Boulder, Colorado, pp. 41-56.
- Royden, L.H., 1993. Evolution of retreating subduction boundaries formed during continental collision. *Tectonics* 12, 629-638.
- Schellart, W.P., Freeman, J., Stegman, D.R., Moresi, L., May, D., 2007. Evolution and diversity of subduction zones controlled by slab width. *Nature* 446, 308-311.
- Schellart, W.P., Lister, G.S., 2004. Tectonic models for the formation of arc-shaped convergent zones and backarc basins. *Geological Society of America Special Papers* 383, 237-258.
- Schellart, W.P., Lister, G.S., Toy, V.G., 2006. A Late Cretaceous and Cenozoic reconstruction of the Southwest Pacific region: Tectonics controlled by subduction and slab rollback processes. *Earth-Science Reviews* 76, 191-233..
- Schmidt, P.W., 1988. A rapid Carboniferous polar shift of New England from palaeomagnetism, in: Kleeman, J.D. (Ed.), *New England Orogen : Tectonics and metallogenesis*. University of New England, Armidale, New South Wales, Australia, pp. 192-198.
- Shaanan, U., Rosenbaum, G., Li, P., Vasconcelos, P., 2014. Structural evolution of the Early Permian Nambucca Block (New England Orogen, eastern Australia) and implications for oroclinal bending. *Tectonics* 33, 1425–1443.
- Shaanan, U., Rosenbaum, G., Wormald, R., 2015. Provenance of the Early Permian Nambucca Block (eastern Australia) and implications for the role of trench

retreat in accretionary orogens. *Geological Society of America Bulletin* 127, 1052-1063.

Shaw, S.E., Flood, R.H., 1981. The New England Batholith, eastern Australia - Geochemical variations in time and space. *Journal of Geophysical Research* 86, 530-

544. Stegman, D.R., Freeman, J., Schellart, W.P., Moresi, L., May, D., 2006.

Influence of trench width on subduction hinge retreat rates in 3-D models of slab rollback. *Geochemistry Geophysics Geosystems* 7.

Torsvik, T.H., 1986. Interactive analysis of palaeomagnetic data. IAPD User Guide:

University of Bergen, Bergen, p. 1-74.

Veevers, J.J., Conaghan, P.J., Powell, C.M., Cowan, E.J., McDonnell, K.L., Shaw, S.E., 1994.

Eastern Australia, in: Veevers, J.J., Powell, C.M.A. (Eds.), *Permian-Triassic*

Pangean basins and foldbelts along the Panthalassan margin of

Gondwanaland. Geological Society of America, Boulder, Colorado, pp. 11-172.

Weil, A.B., Gutierrez-Alonso, G., Johnston, S.T., Pastor-Galan, D., 2013. Kinematic constraints on buckling a lithospheric-scale orocline along the northern margin of Gondwana: A geologic synthesis. *Tectonophysics* 582, 25-49.

Woodward, N.B., 1995. Thrust systems in the Tamworth zone, southern New England

Orogen, New South Wales. *Australian Journal of Earth Sciences* 42, 107-117.

Xiao, W.J., Huang, B.C., Han, C.M., Sun, S., Li, J.L., 2010. A review of the western part of the Altaids: A key to understanding the architecture of accretionary orogens.

Gondwana Research 18, 253-273.

FIGURE CAPTIONS

Figure 1. Simplified 3D illustration of two alternative hypotheses for oroclinal bending (not to scale). (a) Oroclinal bending that is controlled by lithospheric buckling associated with orogen-parallel contraction (after Gutiérrez-Alonso et al., 2004). (b) Oroclinal bending that is controlled by a retreating subduction zone.

Figure 2. Simplified maps of the study area. (a) Major tectonic components of eastern Australia. (b) Geological map of the southern New England Orogen.

Figure 3. Maps and Time-Space diagram highlighting late Paleozoic to early Mesozoic extensional and contractional deformational events in eastern Australia. (a) Geological features associated with pre ~272 Ma regional extension, (b) subsequent Hunter Bowen contractional deformation, and (c) Time-Space diagram. Abbreviations: Gl—Gloucester syncline, Dy—Dyamberin Block, Na—Nambucca Block, Ma—Manning Basin, D'A—D'Aguilar metamorphic complex, Wo—Wongwibinda metamorphic complex, Ti—Tia metamorphic complex. Data sources: (1) Carboniferous subduction complex in the New England (Leitch, 1974; Murray et al., 1987; Glen, 2005). (2) Deposition and distribution of the Sydney, Gunnedah and Bowen basins (Powell et al., 1990; Veevers et al., 1994; Korsch et al., 2009a). (3) Exhumation and cooling of metamorphic complexes in the northern New England Orogen (Little et al., 1992; Holcombe and Little, 1994; Little et al., 1995). (4) S-type plutons in North D'Aguilar Block (310-306 Ma; Little et al., 1995). (5) Meandarra gravity ridge (Korsch et al., 2009a; Krassay et al., 2009). (6) Peak metamorphism in the southern New England Orogen (~296 Ma, amphibolite-facies; Craven et al., 2012). (7) Emplacement of

Urannah Suite batholith (Connors Arch) and associated late stage dykes (308-284 Ma; Allen et al., 1998). (8) Early Permian extensional faults and associated inferred extension directions in and along the Sydney, Gunnedah and Bowen basins (Hammond, 1987; Korsch et al., 2009a; Brooke-Barnett and Rosenbaum, 2015). (9) Early Permian basins in the New England Orogen (Li et al., 2015; Shaanan et al., 2015). (10) Felsic dykes in the Urannah Suite (285 Ma; Allen, 2000). (11) Early Permian emplacement of S-type granitoids (Bundarra and Hillgrove Plutonic Suites) in the southern New England Orogen (Flood and Shaw, 1977; Cawood et al., 2011a; Jeon et al., 2012; Rosenbaum et al., 2012). (12) SHRIMP zircon ages from the Cranky Corner Basin (287 to 284 Ma; Korsch et al., 2009a). (13) Initiation of thermal relaxation subsidence in the Sydney, Gunnedah and Bowen basins (Korsch et al., 2009a). (14) Emplacement of the Alum Mountain Volcanics and Werrie Basalt (271.8 ± 1.8 and 266.4 ± 3.0 Ma respectively; Li et al., 2014). (15) Folded Early Permian strata in the southern New England Orogen (Collins, 1991) and D_2 folds and corresponding penetrative fabric in Nambucca Block (275-265 Ma; Shaanan et al., 2014). (16) Middle Permian to 220-230 Ma folds in the in the northern New England Orogen (Fergusson et al., 1990, 1993; Holcombe et al., 1997). (17) Middle Permian to Triassic cleavage in the northern New England Orogen (Fergusson et al., 1990, 1993; Li et al., 2015). (18) 263—261 Ma folds in the Gunnedah Basin (Veevers et al., 1994). (19) Uplift by faulting of metamorphic complexes in the southern New England Orogen (266-258 Ma; Landenberger et al., 1995). (20) Commencement of thrusting in the Fitzroy region (265 Ma; Holcombe et al., 1997). (21) Post 265 Ma (D_3 and D_4) folds in Nambucca Block (Offler and Foster, 2008; Shaanan et al., 2014). (22) Late Permian to Late Triassic thrust sheet in the Bowen Basin and the Gogango Overfolded Zone (Fergusson, 1991; Fielding

et al., 1997; Holcombe et al., 1997). (23) Late Permian to Late Triassic folds in the Bowen Basin (Fergusson, 1991; Holcombe et al., 1997). (24) Mafic dykes in the Urannah Suite, northernmost New England Orogen (273–229 Ma; Allen, 2000). (25) Thrust-fold of North Pine Fault (Mt Mee) at ~260 Ma and Late-Permian to Triassic thrusts in Marlborough-Fitzroy area, northern New England Orogen (Holcombe et al., 1997). (26) Major final movement on the Peel Fault (latest Permian and before 250 Ma) (Woodward, 1995; Cawood, 2005). (27) I-type plutonism in the southern New England Orogen (255–240 Ma; Shaw and Flood, 1981; Bryant et al., 1997; Cawood et al., 2011b). (28) Minimum constraints of 260 Ma and 241 Ma for activity of thrusts in the western margin of the North D'Aguilar Block (Holcombe et al., 1997). (29) A gap in magmatic activity (Caprarelli and Leitch, 1998; Cawood et al., 2011b).

Figure 4. Geological map and cross sections of the study area (Gloucester and Myall synclines). Sampling sites that were paleomagnetically unstable or inconsistent are in grey. The stereographic projection (equal area lower hemisphere) shows poles to bedding from the Permian succession of the Gloucester syncline. Poles are divided into northern (black and β_n , $n=83$), Central (grey and β_c , $n=28$) and southern (brown and β_s , $n=54$) domains. Dashed line is best-fit girdle for the axial plane of the syncline.

Locations of cross sections are shown in section a.

Figure 5. Photomicrographs of representative lithologies of the Alum Mountain Volcanics. Left sections are taken under cross-polarised light and right sections are under plane-polarised light. For locations see Figure 4. (a) Pumpellyite amygdule in fine mafic groundmass (site G3). (b) Trachyte with sanidine feldspar crystals showing carlsbad twinning and trachytic flow texture (site G21). (c) Rhyolitic ignimbrite with

glassy groundmass and abundant lithic fragments (site G6). (d) Volcanic glass with perlitic texture from the base of the volcanic succession (Site VG in Fig. 4d and corresponding location in 4a).

Figure 6. Alternating field (a), thermal (b), and (c) combined alternating field and thermal demagnetizations. In orthogonal plots, open (closed) symbols show magnetisation vector endpoints in the vertical (horizontal) plane. Stereoplots (Lambert projection) show tilt corrected pointing palaeomagnetic directions (all downwards). Curves show intensities during stepwise demagnetization.

Figure 7. Fold test for paleomagnetic data from the Gloucester and Myall synclines. (a) Stereoplot of in situ mean directions of sampling sites (see also Table 1). (b) Stereoplot of mean directions of sampling sites after tilt correction. (c) Fisher's precision parameter during unfolding.

Figure 8. Paleogeographic reconstructions of the blocks of the southern New England Orogen (T – Texas, NT – North Tamworth, R – Rouchel, G – Gresford, M – Myall, H – Hastings). Paleopoles are shown with circles of confidence: square – mean Gondwanan pole (recalculated from McElhinny et al., 2003 and Cawood et al., 2011b), triangle – mean North Tamworth pole (calculated by Cawood et al., 2011b), circle – Myall pole (this study). (a) After Cawood et al. (2011b). (b) with all block at their present positions with respect to Australia.

Table 1. Alum Mountain Volcanics, paleomagnetic data.

Footnote:

N/n =number of demagnetized/used specimens for calculation samples (sites); D_g , I_g =remanence declination, inclination *in situ*; D_s , I_s =remanence declination, inclination after tilt correction; k =Fisher's precision parameter; α_{95} = the semi-angle of the 95% cone of confidence; VGP = virtual geomagnetic pole (only for the tilt corrected data); d_p , d_m =the semi-axes of the cone of confidence about the pole at the 95% probability level; A_{95} = the semi-angle of the 95% cone of confidence for the VPGs' distribution.

ACCEPTED MANUSCRIPT

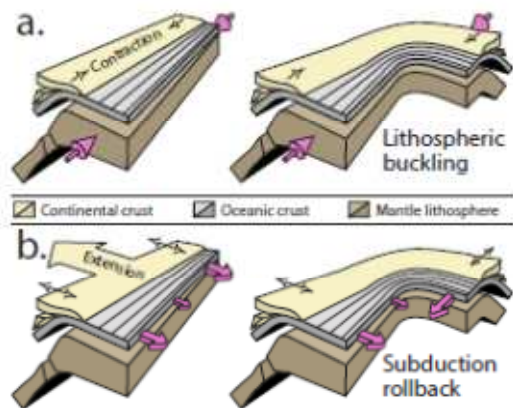


Figure 1. Simplified 3D illustration of two alternative hypotheses for oroclinal bending (not to scale). (a) Oroclinal bending that is controlled by lithospheric buckling associated with orogen-parallel contraction (after Gutiérrez-Alonso et al., 2004). (b) Oroclinal bending that is controlled by a retreating subduction zone.

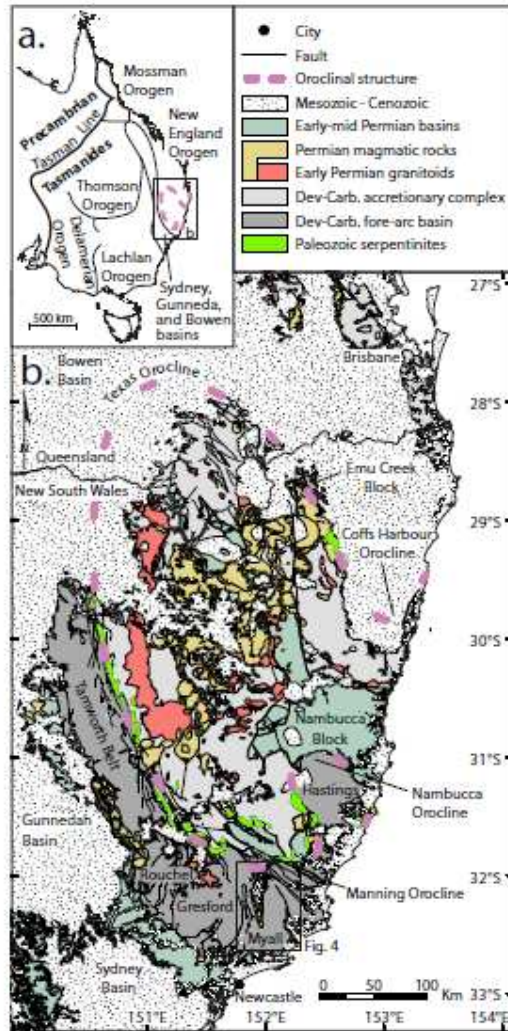


Figure 2. Simplified maps of the study area. (a) Major tectonic components of eastern Australia. (b) Geological map of the southern New England Orogen.

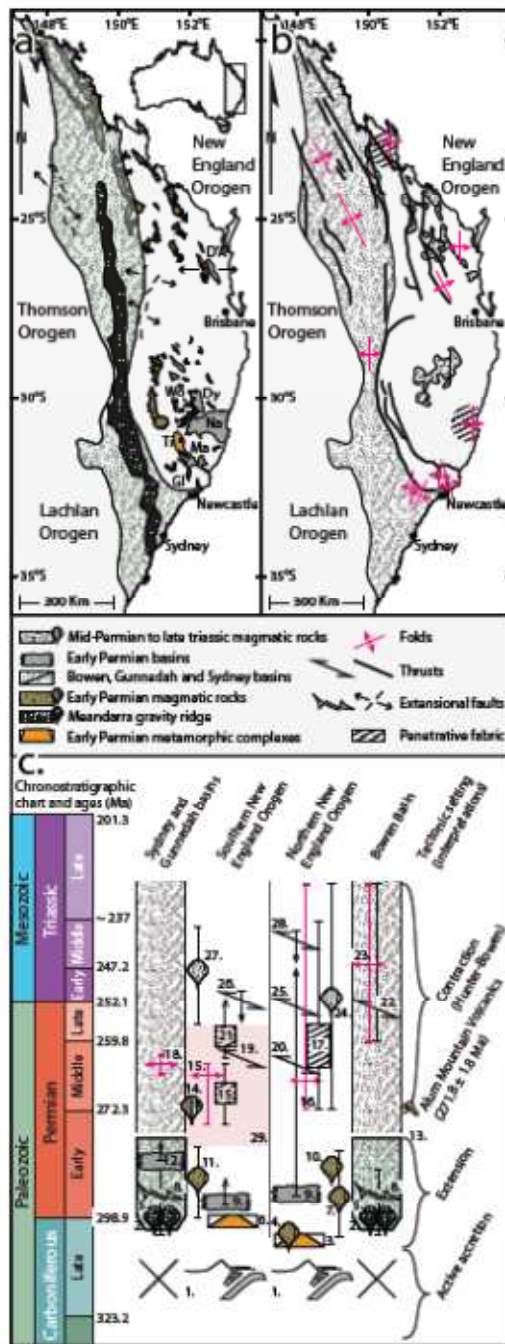


Figure 3. Maps and Time-Space diagram highlighting late Paleozoic to early Mesozoic extensional and contractional deformational events in eastern Australia. (a) Geological features associated with pre ~272 Ma regional extension, (b) subsequent Hunter Bowen contractional deformation, and (c) Time-Space diagram. Abbreviations: GI—Gloucester syncline, Dy—Dyamberin Block, Na—Nambucca Block, Ma—Manning Basin, D'A—D'Aguilar metamorphic complex, Wo—Wongwibinda metamorphic complex, Ti—Tia metamorphic complex. Data sources: (1) Carboniferous subduction complex in the New England (Leitch, 1974; Murray et al., 1987; Glen, 2005). (2) Deposition and distribution of the Sydney, Gunnedah

and Bowen basins (Powell et al., 1990; Veevers et al., 1994; Korsch et al., 2009a). (3) Exhumation and cooling of metamorphic complexes in the northern New England Orogen (Little et al., 1992; Holcombe and Little, 1994; Little et al., 1995). (4) S-type plutons in North D'Aguilar Block (310-306 Ma; Little et al., 1995). (5) Meandarra gravity ridge (Korsch et al., 2009a; Krassay et al., 2009). (6) Peak metamorphism in the southern New England Orogen (~296 Ma, amphibolite-facies; Craven et al., 2012). (7) Emplacement of Urannah Suite batholith (Connors Arch) and associated late stage dykes (308-284 Ma; Allen et al., 1998). (8) Early Permian extensional faults and associated inferred extension directions in and along the Sydney, Gunnedah and Bowen basins (Hammond, 1987; Korsch et al., 2009a; Brooke-Barnett and Rosenbaum, 2015). (9) Early Permian basins in the New England Orogen (Li et al., 2015; Shaanan et al., 2015). (10) Felsic dykes in the Urannah Suite (285 Ma; Allen, 2000). (11) Early Permian emplacement of S-type granitoids (Bundarra and Hillgrove Plutonic Suites) in the southern New England Orogen (Flood and Shaw, 1977; Cawood et al., 2011a; Jeon et al., 2012; Rosenbaum et al., 2012). (12) SHRIMP zircon ages from the Cranky Corner Basin (287 to 284 Ma; Korsch et al., 2009a). (13) Initiation of thermal relaxation subsidence in the Sydney, Gunnedah and Bowen basins (Korsch et al., 2009a). (14) Emplacement of the Alum Mountain Volcanics and Werrie Basalt (271.8 ± 1.8 and 266.4 ± 3.0 Ma respectively; Li et al., 2014). (15) Folded Early Permian strata in the southern New England Orogen (Collins, 1991) and D2 folds and corresponding penetrative fabric in Nambucca Block (275-265 Ma; Shaanan et al., 2014). (16) Middle Permian to 220-230 Ma folds in the in the northern New England Orogen (Fergusson et al., 1990, 1993; Holcombe et al., 1997). (17) Middle Permian to Triassic cleavage in the northern New England Orogen (Fergusson et al., 1990, 1993; Li et al., 2015). (18) 263–261 Ma folds in the Gunnedah Basin (Veevers et al., 1994). (19) Uplift by faulting of metamorphic complexes in the southern New England Orogen (266-258 Ma; Landenberger et al., 1995). (20) Commencement of thrusting in the Fitzroy region (265 Ma; Holcombe et al., 1997). (21) Post 265 Ma (D3 and D4) folds in Nambucca Block (Offler and Foster, 2008; Shaanan et al., 2014). (22) Late Permian to Late Triassic thrust sheet in the Bowen Basin and the Gogango Overfolded Zone (Fergusson, 1991; Fielding et al., 1997; Holcombe et al., 1997). (23) Late Permian to Late Triassic folds in the Bowen Basin (Fergusson, 1991; Holcombe et al., 1997). (24) Mafic dykes in the Urannah Suite, northernmost New England Orogen (273–229 Ma; Allen, 2000). (25) Thrust-fold of North Pine Fault (Mt Mee) at ~260 Ma and Late-Permian to Triassic thrusts in Marlborough-Fitzroy area, northern New England Orogen (Holcombe et al., 1997). (26) Major final movement on the Peel Fault (latest Permian and before 250 Ma) (Woodward, 1995; Cawood, 2005). (27) I-type plutonism in the southern New England Orogen (255-240 Ma; Shaw and Flood, 1981; Bryant et al., 1997; Cawood et al., 2011b). (28) Minimum constraints of 260 Ma and 241 Ma for activity of thrusts in the western margin of the North D'Aguilar Block (Holcombe et al., 1997). (29) A gap in magmatic activity (Caprarelli and Leitch, 1998; Cawood et al., 2011b).

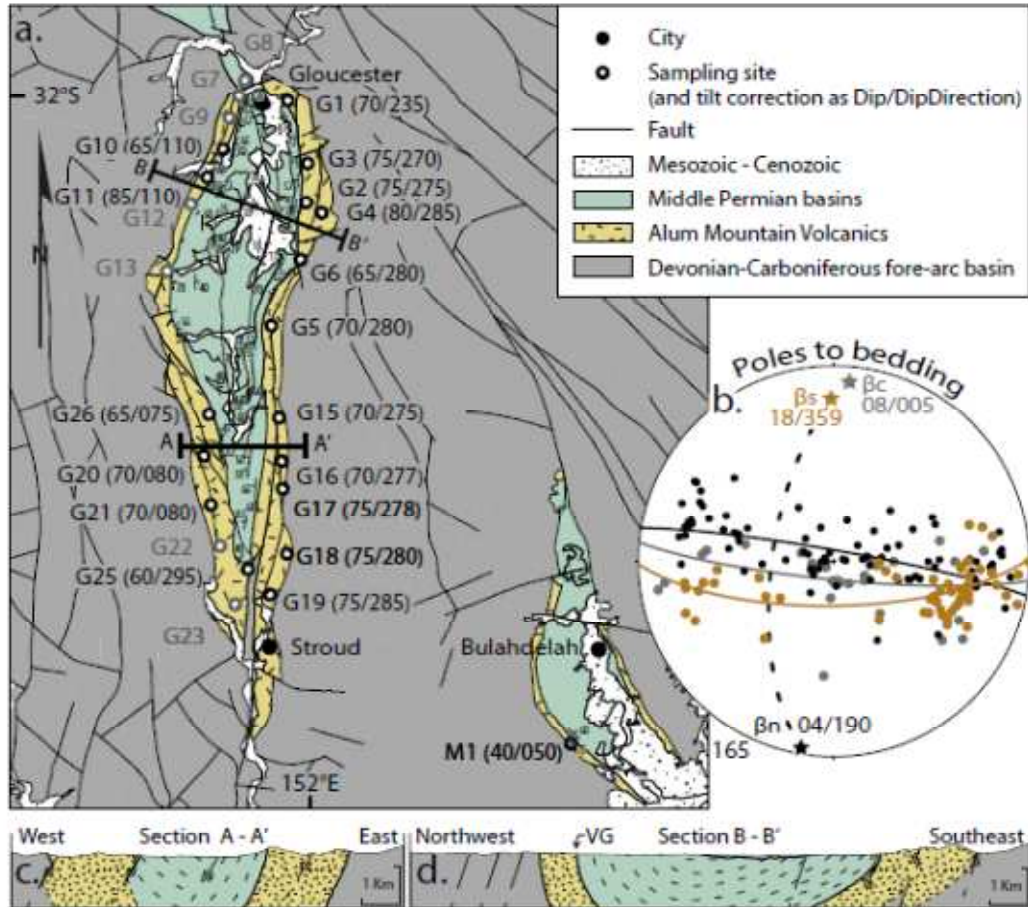


Figure 4. Geological map and cross sections of the study area (Gloucester and Myall synclines). Sampling sites that were paleomagnetically unstable or inconsistent are in grey. The stereographic projection (equal area lower hemisphere) shows poles to bedding from the Permian succession of the Gloucester syncline. Poles are divided into northern (black and β_n , $n=83$), Central (grey and β_c , $n=28$) and southern (brown and β_s , $n=54$) domains. Dashed line is best-fit girdle for the axial plane of the syncline. Locations of cross sections are shown in section a.

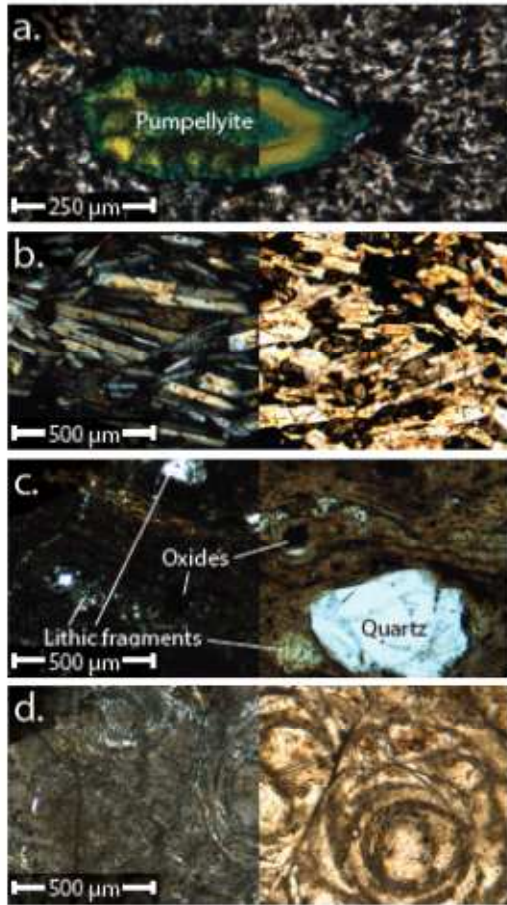


Figure 5. Photomicrographs of representative lithologies of the Alum Mountain Volcanics. Left sections are taken under cross-polarised light and right sections are under plane-polarised light. For locations see Figure 4. (a) Pumpellyite amygdule in fine mafic groundmass (site G3). (b) Trachyte with sanidine feldspar crystals showing carlsbad twinning and trachytic flow texture (site G21). (c) Rhyolitic ignimbrite with glassy groundmass and abundant lithic fragments (site G6). (d) Volcanic glass with perlitic texture from the base of the volcanic succession (Site VG in Fig. 4d and corresponding location in 4a).

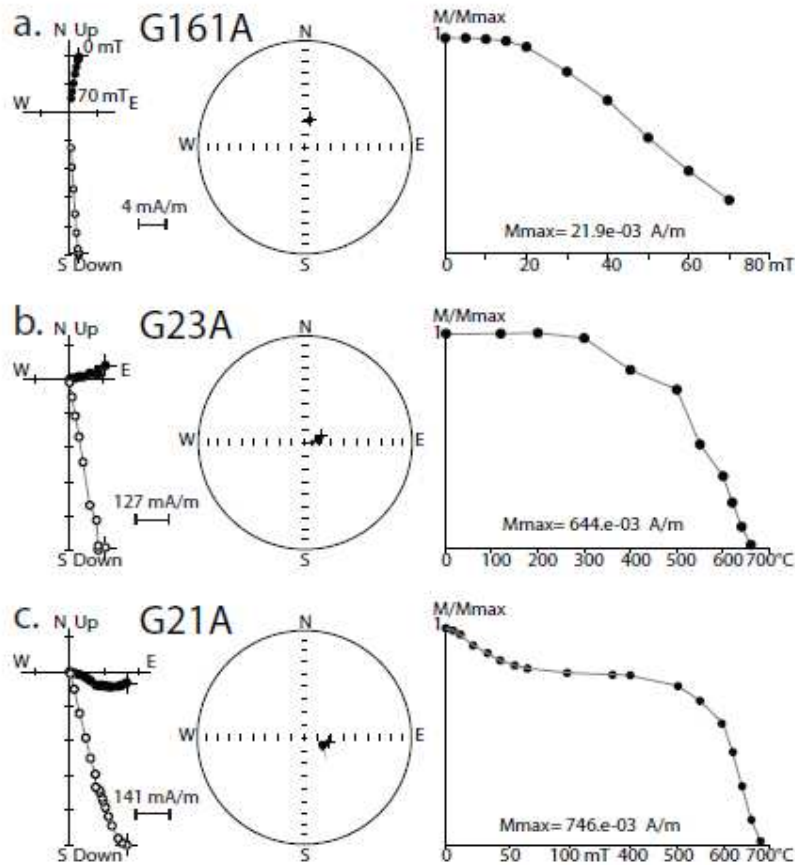


Figure 6. Alternating field (a), thermal (b), and (c) combined alternating field and thermal demagnetizations. In orthogonal plots, open (closed) symbols show magnetisation vector endpoints in the vertical (horizontal) plane. Stereoplots (Lambert projection) show tilt corrected pointing palaeomagnetic directions (all downwards). Curves show intensities during stepwise demagnetization.

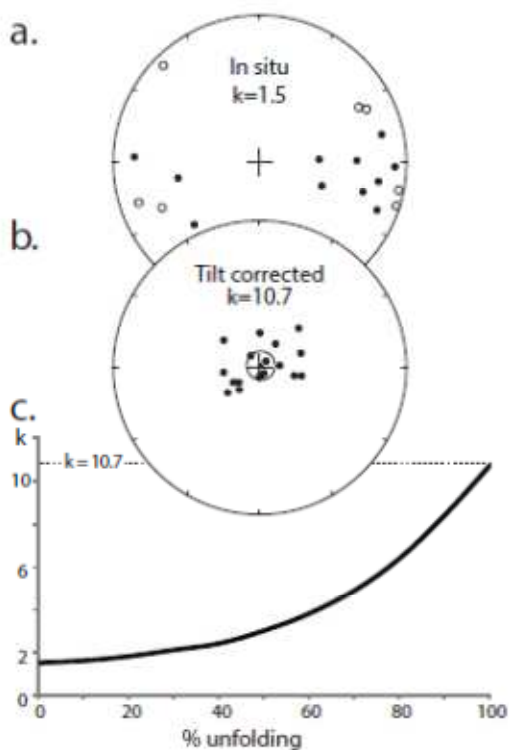


Figure 7. Fold test for paleomagnetic data from the Gloucester and Myall synclines. (a) Stereoplot of in situ mean directions of sampling sites (see also Table 1). (b) Stereoplot of mean directions of sampling sites after tilt correction. (c) Fisher's precision parameter during unfolding.

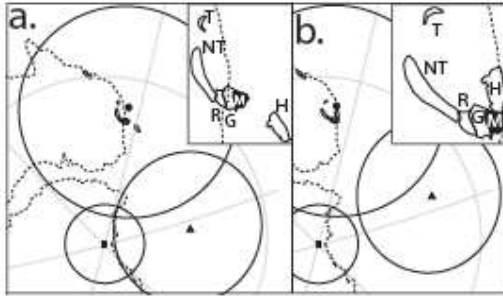


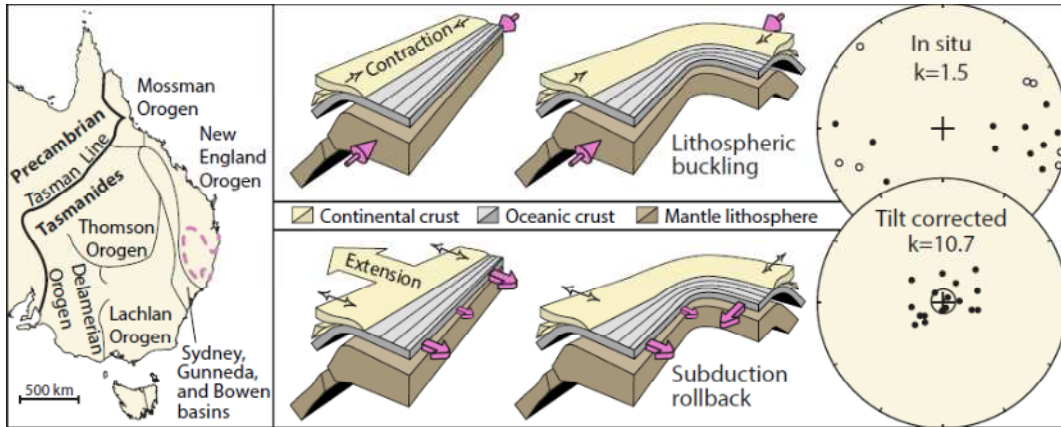
Figure 8. Paleogeographic reconstructions of the blocks of the southern New England Orogen (T – Texas, NT – North Tamworth, R – Rouchel, G – Gresford, M – Myall, H – Hastings). Paleopoles are shown with circles of confidence: square – mean Gondwanan pole (recalculated from McElhinny et al., 2003 and Cawood et al., 2011b), triangle – mean North Tamworth pole (calculated by Cawood et al., 2011b), circle – Myall pole (this study). (a) After Cawood et al. (2011b). (b) with all block at their present positions with respect to Australia.

ACCEPTED MANUSCRIPT

TABLE 1

Site	Location		N/n	Dg	I _g	k	α_{95}	D _s	I _s	k	α_{95}	VGP		dp	dm
	Lat (°S)	Long (°E)										(°N)	(°E)		
G1	32°0'13.85"	151°58'54.16"	7/7	63.6	-11.9	20.4	13.7	70.5	57.0	20.4	13.7	-5.7	200.6	14.5	19.9
G2	32°4'42.56"	151°59'47.34"	7/7	99.1	11.4	59.1	7.8	143.4	84.6	59.1	7.8	-40.4	160.4	15.4	15.6
G3	32°2'59.62"	151°59'49.64"	9/8	61.0	-14.7	32.5	9.9	44.7	48.7	32.5	9.9	15.1	191.3	8.6	13.0
G4	32°5'9.81"	152°0'36.10"	7/7	112.1	8.5	373.6	3.1	183.5	82.8	373.6	3.1	-46.2	150.8	5.9	6.1
G5	32°10'2.74"	151°58'3.37"	7/3	105.9	17.7	1492.0	3.2	168.6	84.0	1492.0	3.2	-43.8	155.2	6.2	6.3
G6	32°7'10.61"	151°59'30.79"	9/9	101.3	-2.0	124.2	4.6	102.9	63.0	124.2	4.6	-30.5	205.8	5.7	7.2
G10	32°2'23.02"	151°55'32.90"	8/7	272.5	8.9	60.5	7.8	241.0	66.8	60.5	7.8	-42.1	101.8	10.6	12.9
G11	32°3'35.62"	151°54'43.94"	9/8	315.0	-4.2	347.4	3.0	0.2	63.4	347.4	3.0	13.0	152.1	3.7	4.7
G15	32°14'5.55"	151°58'26.36"	10/6	91.9	4.7	90.4	7.1	83.4	74.4	90.4	7.1	-24.7	182.4	11.7	12.9
G16	32°16'0.39"	151°58'35.12"	6/6	77.2	9.2	20.6	15.1	33.6	68.0	20.6	15.1	1.5	172.3	21.3	25.3
G17	32°17'7.78"	151°58'37.28"	11/11	89.0	23.0	108.9	4.4	323.4	78.3	108.9	4.4	-13.5	138.4	7.8	8.3
G18	32°20'1.29"	151°58'47.77"	9/8	110.7	41.4	321.2	3.1	262.7	62.0	321.2	3.1	-26.4	98.2	3.7	4.8
G19	32°21'42.24"	151°57'57.44"	7/6	87.2	45.9	75.6	7.8	307.2	55.7	75.6	7.8	5.5	111.8	8.0	11.2
G20	32°15'46.98"	151°54'30.27"	10/8	245.1	-17.5	41.2	8.7	231.7	58.8	41.2	8.7	-48.1	87.0	9.6	13.0
G21	32°17'52.47"	151°54'54.19"	11/11	251.6	-8.0	24.5	9.4	234.8	70.2	24.5	9.4	-45.9	108.6	14.0	16.2
G25	32°20'40.13"	151°56'55.24"	7/6	107.6	-1.4	18.6	16.0	101.0	57.8	18.6	16.0	-27.3	211.9	17.3	23.5
G26	32°13'57.50"	151°54'50.76"	10/4	259.2	30.9	966.1	3.0	43.8	83.0	966.1	3.0	-21.9	162.2	5.7	5.9
M1	32°28'40.74"	152°11'39.22"	6/6	226.6	26.8	246.1	4.3	222.3	66.7	246.1	4.3	-54.5	103.1	5.9	7.1
All sites	32.2°	152.0°	26/18	101.3	25.1	1.5	49.0	27.5	88.2	10.7	11.1	-30.0	153.2	A₉₅ = 19.5°	

N/n=number of demagnetized/used specimens for calculation samples (sites); Dg, I_g=remanence declination, inclination *in situ*; D_s, I_s=remanence declination, inclination after tilt correction; k=Fisher's precision parameter; α_{95} = the semi-angle of the 95% cone of confidence; VGP = virtual geomagnetic pole (only for the tilt corrected data); dp, dm =the semi-axes of the cone of confidence about the pole at the 95% probability level; A₉₅ = the semi-angle of the 95% cone of confidence for the VPGs' distribution.



Graphical abstract

ACCEPTED MANUSCRIPT

Highlights

- A Permian paleopole from the southernmost New England oroclinal was obtained.
- Data show no rotations relative to cratonic Australia/Gondwana after ~272 Ma.
- Oroclinal bending occurred before 272 Ma and prior to the Hunter-Bowen Orogeny.
- The New England oroclinal formed in extensional setting likely by trench retreat.

ACCEPTED MANUSCRIPT